



Paleoearthquakes Determination of Magnitude~6.5 on the North Tehran Fault, Iran

H. Nazari^{1*}, J.-F. Ritz², A. Ghassemi³, K. Bahar-Firouzi³, R. Salamati³, A. Shafei³, and M. Fonoudi³

1. Research Institute for Earth Sciences, Geological Survey of Iran, Iran and Géosciences Montpellier, UMR 5243, CNRS, Université Montpellier, France,

* Corresponding Author; email: h.nazari@gsi.ir

2. Géosciences Montpellier, UMR 5243, CNRS, Université Montpellier, France

3. Geological Survey of Iran, Iran

ABSTRACT

The North Tehran Fault is located at the southernmost piedmont of Central Alborz, north of Iran. It stands out as a major active fault menacing directly the city of Tehran, a 12 million people metropolis, and would have been the source of several major historical earthquakes in the past. The fault zone extends up to 110km and corresponds mainly to a reverse fault mostly crossing the northern suburbs of the Tehran metropolis, although NTF in its eastern part is characterized more as a left lateral strike slip active fault. We carried out a paleoseismological study of the fault zone in order to determine whether the fault was activated during the Holocene, and to define the characteristics of its activity in terms of kinematics and magnitude. Here in this paper we present only a part of our paleoseismological investigations trench TE2. Observations from two trenches dug across the North Tehran fault scarp reveal evidence for a maximum of six surface-rupturing events within the late quaternary. According to the empirical relationships among average displacement per event and Moment magnitude [25], we can estimate six events $M_w \sim 6.5$ associated with these ruptures in TE2 trench.

Keywords:

Iran; Alborz;
North Tehran fault;
Paleoseismology

1. Introduction

The North Tehran Fault is located along the Central Alborz and Tehran plain border, see Figures (1) and (2). It was the subject of several investigations [e.g. 1-10], and it has been described by all the authors as a thrust fault juxtaposing volcano-sedimentary Paleogene series on Plio-Quaternary detritus sediments. The North Tehran Fault extends over approximately 110km, with a general “V” concave shape trace to the North at the surface, switching from the NW-SE direction to NE-SW between the cities of Karadj and Tehran. The fault trace is, however, difficult to follow - mainly because of urban development - and it appears to be divided into several splays, Figures (3) [5, 8].

However, despite numerous historical seismicity data (i.e. 793AD, 853AD, 855AD, 864AD, 898AD, 1177AD, 1384AD, 1847AD and 1868AD) [11-13], see Figure (1), the activity of these faults or even

that of the North Tehran Fault has not been well known, and the question of whether these faults correspond to deep-seated faults or if they correspond to a fold and thrust system within the alluvial piedmont absorbing the displacement along the main North Tehran is not resolved, see Figures (2) and (3).

2. Tectonic Setting

The elevation of the mountain peaks immediately to the north of Tehran (i.e. Tochal 3957m) from the fault may exceed 2500m, see Figure (2).

Allen et al [14] suggest that the North Tehran Fault is deeply rooted in the crust (“deep-seated fault”). According to a structural model based on the restoration of Central Alborz structures at the Eocene, Nazari [15] interprets the North Tehran Fault as the reactivation by inversion of an ancient

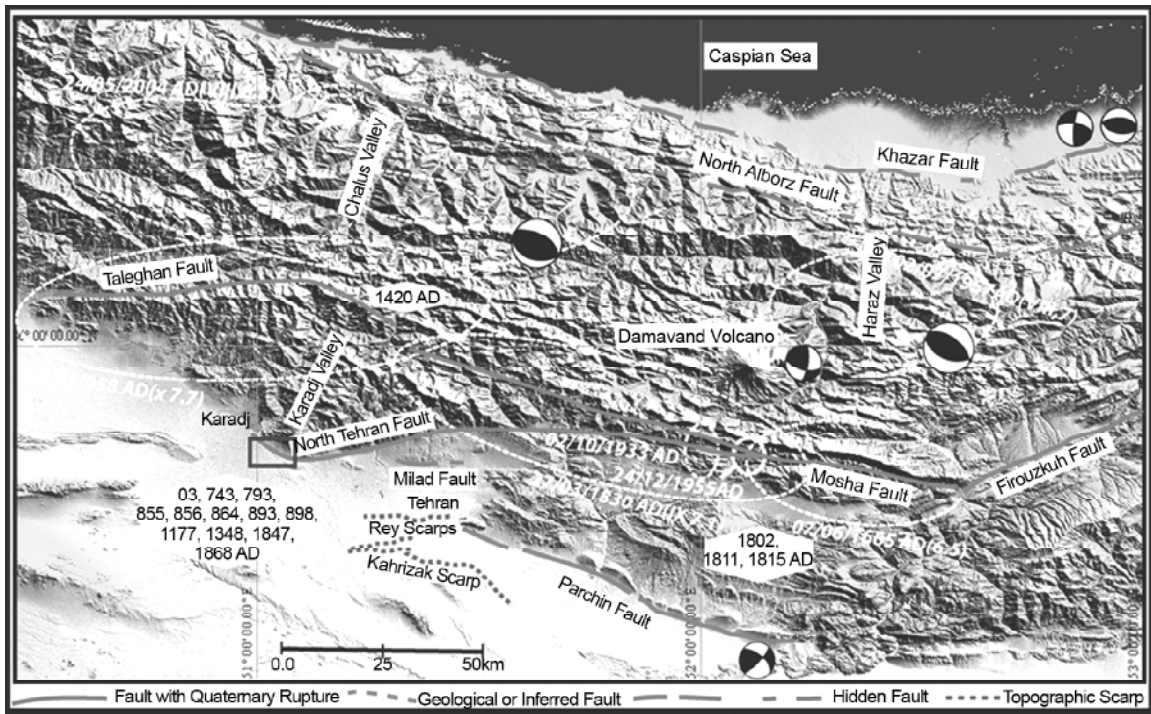


Figure 1. Seismotectonic sketch map of Central Alborz: White dashed circles represent the epicentral areas and dates of historical earthquakes; dates inside the white diamond correspond to historical earthquakes that damaged the Tehran/Rey area after [12, 13, 19]. Focal mechanisms of instrumental earthquakes after [26-28]. Black rectangle approximately is corresponding to the paleoseismological studied sites and back ground image is SRTM data with position resolution 90m.

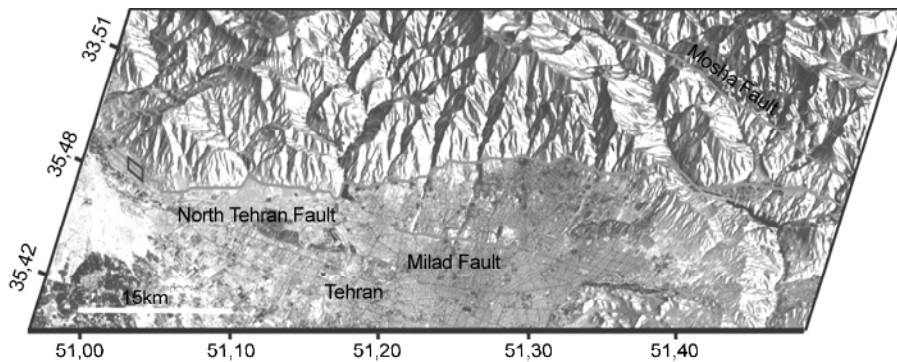


Figure 2. North Tehran fault (light grey line) shown on Digital elevation model derived from Aster satellite image. The black frame defines the studied area shown in Figure (1).

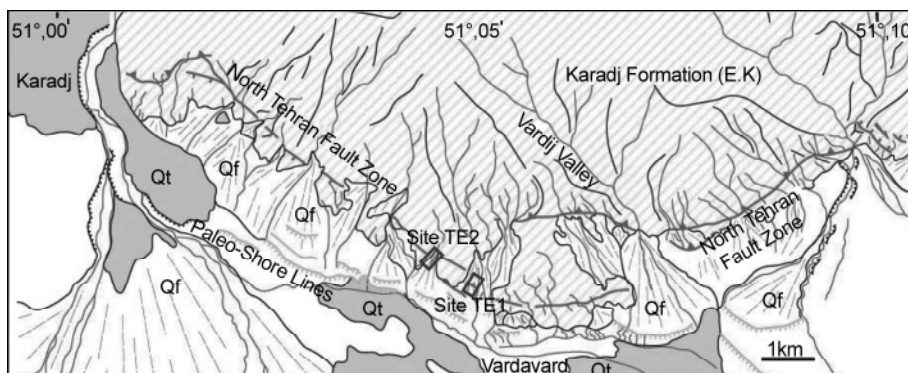


Figure 3. Detailed Cartography maps of western part of the North Tehran Fault between Tehran in the east and Karaj in the west. Thick grey lines show the North Tehran Fault zone and light grey ones define shorelines; paleoseismological sites, TE1 and TE2 shown by rectangles.

Eocene normal fault that connects a major structure of lithospheric scale, namely the Mosha Fault, along which the main left-lateral shear across Central Alborz is taken [16-17].

One of the “classical” outcrops [5] where the North Tehran Fault can be observed, showing the Karadj volcano-sedimentary formations overlapping the alluvium that are attributed to the Plio-Quaternary, is at the entry of Kan Valley. However, these deformations do not represent the active North Tehran Fault since the youngest (probably Holocene) deposits seal the overlapping contacts.

In the south of the North Tehran Fault, the alluvial sediments have been affected by the fault in several places, defining secondary structures (e.g. Milad, Niavaran and Mahmoudieh faults), see Figures (1), (2), and (4). These structures can be interpreted as folds controlled by thrusts faults, called Forebergs [18].

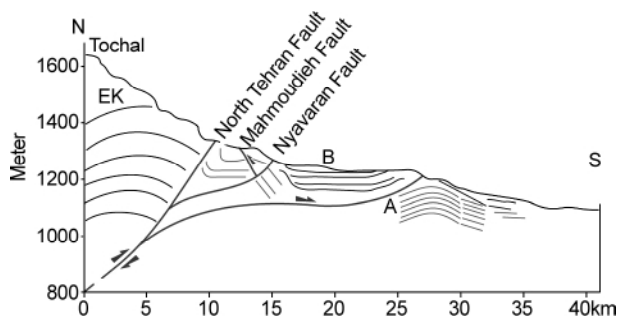


Figure 4. Schematic cross-section of the North Tehran fault zone: EK: Karadj Formation, A: Hezardareh formation, B: Tehran Alluvium (modified after 2).

The North Tehran Fault joins the Mosha Fault in the East, while in the West it turns to Abyek Fault likely involving the same kinematics [19], the Abyek Fault joins in turn the North Qazvin Fault. We conceive the faults of North Tehran, Abyek and North Qazvin as belonging to the same shear zone of primarily reverse kinematics - with a small left lateral component - along which part of the shortening of Central Alborz has been absorbed. Since Miocene, this fault zone seems to have worked in compression mode - while it behaved as normal fault before Miocene [15, 20]. This compression seems to have remained always localised, mainly on the same major structure, except in the area of Tehran where one observes more frontal structures corresponding, in particular, to fault propagation folds in recent quaternary series. Less

than 1mm/y estimated slip rate for the North Tehran fault [8], could be interpreted as a sign of its long-term return seismic activity in the late of quaternary.

3. Paleoseismology of the North Tehran Fault

By means of a morphotectonic analysis, we identified some of the recent activities of the North Tehran Fault, in particular, between Tehran and Karadj [8, 15]. In this zone, at the southern side of the Nowlat Mountain, see Figures (2) and (3), the morphology carries seemingly the signature of important landslides corresponding to collapsed rocks of the Karadj formation, see Figure (5). However, aerial photos and field survey allow us to recognize a scarp that offsets vertically a recent colluvial-alluvial surface which should correspond to the units *C* and *D* according to the nomenclature of Tehran alluvium [5], see Figures (5). Two parallel underground galleries of water (Ghanat) cross slightly obliquely the scarp line, see Figures (6) and (7).

We found some evidences of ground ruptures west of the main trench (*TE1*), see Figures (3) and (6), by cleaning an artificial riser (*TE2*), oriented *ESE-WNW*, see Figures (3) and (6). At this site, the original morphology has been largely modified by the human activity, and we could hardly corroborate the ruptures found downstream the section with an escarpment at the surface, see Figures (6) and (7).

The following section presents the description of one of the two studied sites where we opened two

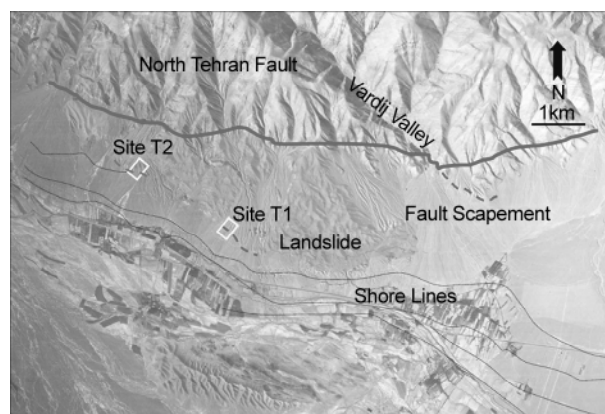


Figure 5. North Tehran fault zone between Tehran and Karaj seen on aerial photo (1:50,000) taken in 1955AD. The main - but not necessarily still active - fault is drawn in thick grey. The studied paleoseismological sites are indicated by rectangles, T1 and T2 as *TE1* and *TE2* in the text. Shaded grey areas correspond to possible landslides. Grey dot lines indicate ancient-shore lines.

trenches *TE1* and *TE2*, both *NS* oriented. We logged the stratigraphic units according to their nature, size of clasts and matrix, as well as their colours with a reference grid of $1m \times 1m$ square at a scale of $1/10^{th}$ with $0.5cm$ accuracy. The analysis of stratigraphy and the structures observed in the two trenches, as well as the retrospective reconstitution of sedimentary events (deposits, erosion) in relationship or not to seismic events, enable us to identify several past earthquakes characterized by “event horizons” corresponding mostly to scarp-derived colluviums (colluvial wedge) burying pre-faulting horizons [e.g. 21-24].



Figure 6. A Quick bird image, Google earth satellite image (<http://www.google earth.com>) of the trench sites, two trenches, *TE2* and *TE3* in north of Garmdareh (shown in Figure (5)); two lines of wells of ghanat are significant by small cone in west of *TE2*. GPS coordinates below the image are corresponded to geographical location of the white flag in south of the trench *TE2*.

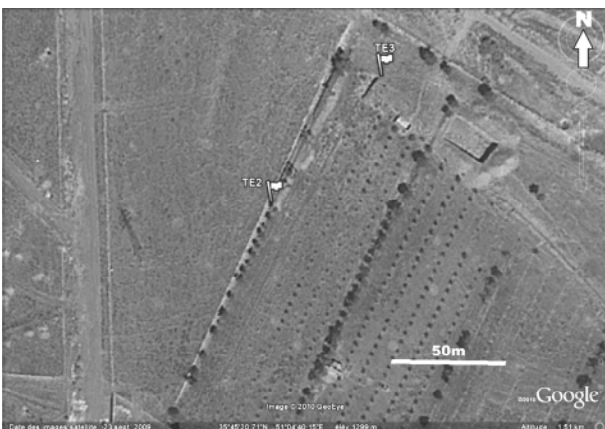


Figure 7. A close-up view of the trenches *TE2* and *TE3* on google satellite image (<http://www.google earth.com>) shown in Figure (6); GPS coordinates below the image are corresponded to geographical location of the blue flag in south of the trench *TE2*.

4. Site *TE2*

As expected from the mapping of the area, the deposits found in the trench *TE2* correspond to colluvial-alluvial material accumulated in successive stratigraphic units at the foothills of the Alborz Mountain. Trench *TE2(T2)* that located at $35^{\circ} 45' 55,31''N$ and $51^{\circ} 04' 09,97''E$ prepared by re-cleaning an artificial riser, face to the east, with $\sim 70m$ long and $3-4m$ high, see Figures (7) and (8). An additional trench (dimensions $12m, 1m, 2.5m$) also excavated immediately ($20m$) to the east of *TE2* through an escarpment visible in the field revealed to be related to human activity (the scarp is following a Ghanat gallery), see Figures (6) and (9).

4.1. Log of the Western Wall of *TE2*

Our paleo-seismological observation on the wall of the trench *TE2* allows us to identify six events, see



Figure 8. Trench *TE2* seen towards the South.



Figure 9. An artificial scarp, view to the east located on the horizontal gallery of the Ghanat that seen in the north part of trench *TE2*.

Figure (10). Five of the events are identified in a fault zone approximately 7m broad located in the southern part of the trench, see Figures (11) and (12) along which the deformation is distributed on four ruptures (F1 to F4), see Figure (13). Another older event is observed nearly 25m farther north, see Figure (12).



Figure 10. A general view to the north of the paleoseismological logged wall of the trench TE2.

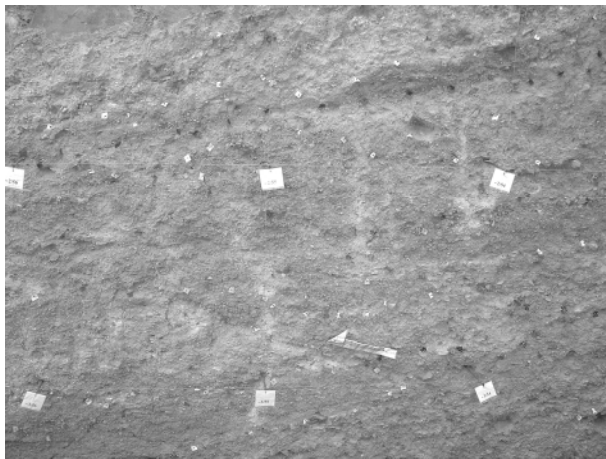


Figure 11. A close-up field photo of the logged wall of TE2, view to the west, located between horizontal grid lines -1 to -3 and vertical lines 54 to 56 in Figure (12).

4.2. The Stratigraphy of the Paleo-Earthquakes Backwards in Time is as Follows

- Event 1-Unit 3: Unit of colluvial wedge intersected by the principal fault and covered by units 11 and 2. The minimum offset of the bottom of unit 3 along the fault F2 is 30 cm, see Figures (12) and (13).
- Event 2-Unit 7: Alluvial unit observed in particular in the footwall south of the trench, eroded in

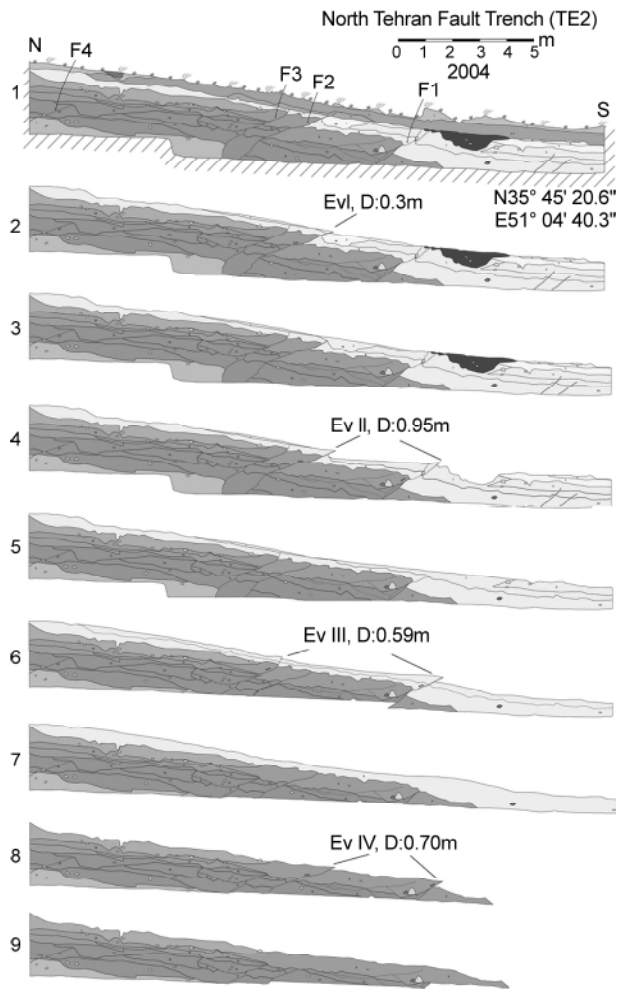


Figure 13. Interpretative retrospective scenario of deposition/ruptures in trench TE2, and log where the stratigraphic units are grouped in main isochrones.

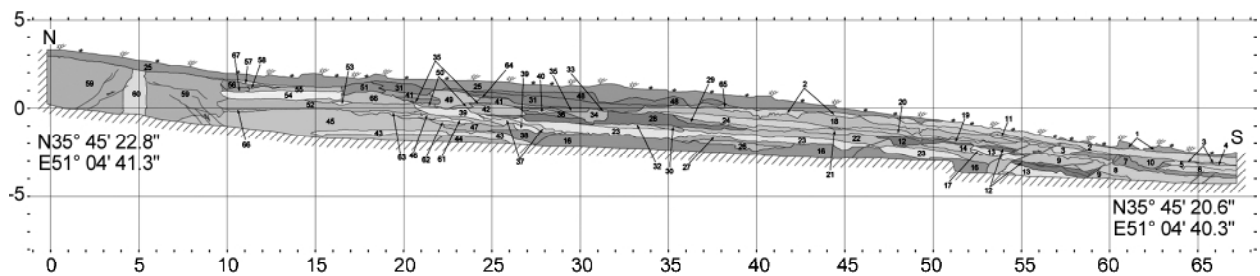


Figure 12. Logs of the western wall in trench TE2: Log with individualization of all stratigraphic units.

the hanging wall. In total, the base of the unit is shifted 95cm (70cm+25cm along two ruptures F2 and F1, respectively). This unit is covered with the colluvial-wedge units 3 and 10 (the base of these two units corresponding to an erosion surface suggests that deposition has taken place in an erosive context), see Figures (12) and (13).

- Event 3-Unit 8: Unit of debris flow whose bottom appears to be shifted approximately 59cm (40cm and 19cm along the rupture planes F1 and F3, respectively), see Figures (12) and (13).
- Event 4-Unit 9: Unit of debris flow along the planes F1 and F2 whose base shows a total displacement of 70cm (50cm and 20cm, respectively), see Figures (12) and (13).
- Event 5- Unit 22 and its isochrones (12, 13, and 14): Unit of debris flow located at the base of the trench and affected along the planes F3 and F4. Being in the limit of observation in the lower part of the trench and given the uncertainty of the log due to the heterogeneity of the deposits, the displacement values can't be estimated, see Figures (12) and (13).
- Event 6-Unit 16: Unit of colluvium-debris flow in the northern part of the trench affected by a reverse fault, see Figure (14). We cannot attribute an exact value to the displacement of unit 16 since, according to our log, it is absent at the hanging wall, certainly as a result of erosion posterior to the event that shifted it. If this interpretation is right, it implies a significant displacement. Let us note that units 43 and 44 appear folded on the hanging wall, see Figure (12).

4.3. Estimation of the Magnitudes, Table (1)

The offsets of the “units-event horizon” can be translated into Magnitude *M_w* of the seismic moment

following the empirical functions of Wells and Coppersmith [25] in the case of a reverse fault and in the general case. In this calculation, we did not take into account the fact that the kinematics of the fault involves a tiny sinistral transverse component. As a result, these estimates provide lower bounds.

Although, we have not geochronological data for the trench TE2, and it is impossible to make a well stratigraphic correlation between TE2 and TE1, [8, 15]. However, it should be mentioned that both of trenches are similar in number of events and their estimated magnitudes as reported by Nazari [15].

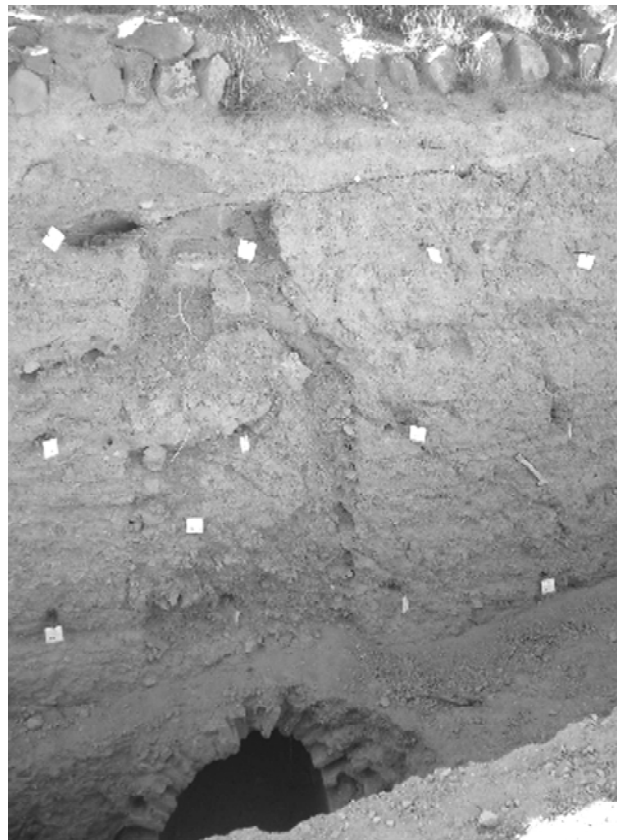


Figure 14. Collapsed Ghanat repaired with bricks and filled up with debris, situated in north part of trench TE2.

Table 1. Values of the magnitudes *M* of paleo-events estimated from MD as maximum displacement from the functions of Wells and Coppersmith [25] in the trench TE2.

N°	F1/Offset (m)	F2/Offset (m)	F3/Offset (m)	F4/Offset (m)	Total Offset (m)	M _w (MD), Reverse	M _w (MD), General
Ev 1	-	0.30	-	-	0.30	6.29	6.30
Ev 2	0.25	0.70	-	-	0.95	6.51	6.67
Ev 3	0.40	-	0.19	-	0.59	6.41	6.52
Ev 4	0.50	0.20	-	-	0.70	6.45	6.58
Ev 5	-	-	-	-	-	-	-
Ev 6	-	-	-	-	-	-	-

In the north of the trench *TE2*, one observes a Ghanat gallery which was destroyed (by a seismic event?), then repaired, see Figures (9) and (14). On both sides of the zone which collapsed, one observes conjugated normal faults. Moreover, the roof of the Ghanat is repaired with bricks on a section on top of which a mass of completely disorganized sediments can be observed (neither stratigraphy nor graded bedding). On top of it, there is a horizontal deposit in which stones have been arranged in the form of an ancient wall.

From our point of view, these observations can be associated with the collapse of an underground gallery related to an earthquake some time ago. After removing the rocks filling the gallery (and the natural trench formed by the collapse), the gallery should have then been repaired with bricks, and the remainder of the trench filled with gravels and loose material. Finally, the ground should have been again disturbed at the time of the construction of the wall observed at the surface.

5. Conclusion

Along the North Tehran fault zone, we identified and characterized an active reverse fault segment with a small sinistral component between the cities of Tehran and Karadj. This segment shows a cumulative deformation involving six paleo-earthquakes which were observed in trench *TE2* of magnitudes M_w from 6.3 to 6.5 as estimated by means of the empirical laws of Wells and Copper-smith [25]. Occurring of these earthquakes could be corresponded to estimated values in Trench *TE1* by Nazari et al [8] and Nazari [15] for the late quaternary seismic activities along the North Tehran Fault as the closest hazardous seismic fault to Iran's capital.

Acknowledgements

This work was supported by a French-Iranian research program on the study of the seismic risk within the Tehran region (coordinator D. Hatzfeld). We are grateful to the Geological Survey of Iran (*GSI*) especially M. Gorashi and A. Saidi, the *CNRS* and the French Embassy in Iran for their support. We thank the members of the *GSI*: M. Talebian, F. Ansari, M. Bolurchi, M. Asad Beigi and A. Karbalai Hasan for their help to logging. We also thank A. Delpinque for drawings and F. Radjaie for his help in English editing.

References

1. Rieben, E.H. (1955). "The Geology of the Tehran Plain", *Am. J. Sci.*, **253**, 617-639.
2. Dresch, J. (1961). "Le Piemont de Teheran, In Observations de Geographie Physique en Iran Septentrional, Centre Docum, Cart. Geogr., Mem. et Docum, 85-101.
3. Knill, J.L. and Jones, K.S. (1968). "Ground Water Condition in Greater Tehran", *Quart. J. Eng. Geol.*, **1**, 181-194.
4. Tchalenko, J.S. (1974). "Recent Destructive Earthquakes in the Central Alborz", *GSI*, **29**, 97-116.
5. Berberian, M., Ghorashi, M., Argangraves, B., and Mohajer Ashjaie, A. (1985). "Seismotectonic and Earthquake Fault Hazard Investigations in the Tehran Region", (In Persian), *GSI*.
6. Abbassi, M.R., Shabanian, E., Farbod, Y., Feghhi, Kh., and Tabassi, H. (2003). "The State of Contemporary Stress in the Southern Flank of Central Alborz" (In Persian), *IIIES*, Tehran, 118p.,
7. Nazari, H., Ritz, J.-F., Salamati, R., Solaymani, S., Balescu, S., Michelot, J.-L., Ghassemi, A., Talebian, M., Lamothe, M., Massault, M., and Ghorashi, M. (2007). "Paleoseismological Analysis in Central Alborz, Iran", *The 1957 Gobi-Altay Earthquake Commemorating Conf.*, Ulaanbaatar-Mongolia.
8. Nazari, H., Ritz, J.-F., Balescu, S., Lamothe, M., Salamati, R., Talebian, M., Ghorashi, M., and Saidi, A. (2008). Paleoseismological Analysis of the North Tehran Fault, Iran, Analysing Prehistoric Ruptures for the Past 30.000 ka, 33IGC, Oslo.
9. Abbassi, M.R. and Farbod, Y. (2009). "Faulting and Folding in Quaternary Deposits of Tehran's Piedmont (Iran)", *Journal of Asian Earth Sciences*, **34**, 522-531.
10. Solaymani Azad, S., Ritz, J.-F., and Abbassi, M. (2011). Left-Lateral Active Deformation along the Mosha-North Tehran fault (Iran): Morphotectonics and Paleoseismological Investigations, *Tectonophysics*, **497**, 1-14.
11. Ambraseys, N.N. and Melville, C.P. (1982). "A History of Persian Earthquakes", Cambridge University Press, New York, 219p.

12. Berberian, M. and Yeats, R.S. (1999). "Patterns of Historical Earthquake Rupture in the Iranian Plateau", *Bulletin of Seismological Society of America*, **89**(1), 120-139.
13. Berberian, M. and Yeats, R.S. (2001). "Contribution of Archeological Data to Studies of Earthquake History in the Iranian Plateau", *J. Struct. Geol.*, **23**, 563-584.
14. Allen, M.B., Ghassemi, M.R., Shahrabi, M., and Qorashi, M. (2003). "Accommodation of Late Cenozoic Oblique Shortening in the Alborz range, northern Iran", *Journal of Structural Geology*, **25**, 659-672.
15. Nazari, H. (2006). "Analyse de la Tectonique Récente et Active Dans l'Alborz Central et la Région de Téhéran: Approche Morphotectonique et Paléoseismologique", Unpublished PhD Thesis, University of Montpellier II, 247p.
16. Ritz, J.-F., Nazari, H., Ghassemi, A., Salamati, R., Shafei, A., Soleymani, S., and Vernant, P. (2006). "Active Transtention Inside Central Alborz: A New Insight into the Northern Iran-Southern Caspian Geodynamics", Accepted in *Geology*.
17. Soleymani Azad, S. (2009). "Evaluation de l'alea Seismique Pour les Villes de Teheran, Tabriz et dans le NW de l'Iran Approche Morphotectonique et Paleoseismologique", Science de la Terre et de L'eau, Ph.D tesis, Montpellier, Montpellier II, 150.
18. Bayasgalan, A.; Jackson, J., Ritz, J.-F., and Carretier, S. (1999). "'Forebergs', Flower Structures, and the Development of Large Intra-Continental Strike-Slip Faults: The Gurvan Bogd Fault System in Mongolia", *Journal of Structural Geology*, **21**, 1285-1302.
19. Berberian, M., Ghorashi, M., Arjangraves, B., and Mohajer Ashjaie, A. (1993). "Seismotectonic and Earthquake-Fault Hazard Investigations in the great Ghazvin Region (in Persian), 61p., GSI.
20. Nazari, H. and Ritz, J.-F. (2008). "Neotectonics in Central Alborz", *Geosciences, GSI*, **17**(1), Special Issue.
21. McCalpin, J.P. (1996). *Paleoseismology*, Academic Press, New York, 588p, ISBN 978-0-12-373576-8.
22. Nazari, H., Ritz, J.-F., Salamati, R., Shafei, A., Ghassemi, A., Michelot, J.-L., Massault, M., and Ghorashi, M. (2009a). "Morphological and Paleoseismological Analysis along the Taleghan Fault (Central Alborz, Iran)", *GJI*, **178**(2), 1028-1041, doi: 10.1111/j.1365-246X.2009.04173.x.
23. Nazari, H., Fattahi, M., Meyer, B., Sebrier, M., Talebian, M., Forootan, M., Le Dortz, K., Bateman, M.D., and Ghorashi, M. (2009b). "First Evidence for Large Earthquakes on the Deshir Fault, Central Iran Plateau", **21**(6), 417-426, doi: 10.1111/j.1365-3121.2009.00892.x.
24. Nazari, H., Ritz, J.-F., Salamati, R., Shahidi, A., Habibi, H., Ghorashi, M., and Talebian, M. (2010). "Distinguishing between Fault Scarps and Shorelines: The Question of the Nature of the Kahrizak, North Rey and South Rey features in Tehran Plain (Iran)", *Terra Nova*, doi: 10.1111/j.1365-3121.2010.00938.x.
25. Wells, D.L. and Coppersmith, K.J. (1994). "Empirical Relationships Among Magnitude, Rupture Length, Rupture Area, and Surface Displacement", *Bull. Seismo. Soc. Am.*, **84**, 974-1002.
26. McKenzie, D.P. (1972). "Active Tectonics of the Mediterranean Region", *Geophys. J. Roy. Astron. Soc.*, **30**, 109-185.
27. Jackson, J., Priestley, K., Allen, M., and Berberian, M. (2002). "Active Tectonics of the South Caspian Basin", *Geophysical Journal International*, **148**, 214-245.
28. Tatar, M., Jackson, J., Hatzfeld, D., and Bergman, E. (2007). The 28 May 2004 Baladeh Earthquake (Mw 6.2) in the Alborz, Iran: Overthrusting the South Caspian Basinmargin, Partitioning of the Oblique Convergence, and Seismic Hazard of Tehran", *Geophys. J. Int.*, **170**, 249-261.